catalysts

MDPI

Article

A Continuous Fixed Bed Adsorption Process for Fez City Urban Wastewater Using Almond Shell Powder: Experimental and Optimization Study

Ibtissame Elmansouri [1,*], Amal Lahkimi [2], Mohammed Kara [2,3,*], Anouar Hmamou [2], Ghita El Mouhri [4], Amine Assouguem [5], Mehdi Chaouch [2], Abdulwahed Fahad Alrefaei [6], Mohamed Kamel [7], Lotfi Aleya [8], Mohamed M. Abdel-Daim [9], Noureddine Eloutassi [2], Abderrazzak Adachi [2] and Hicham Bekkari [1]

1 Laboratory of Environmental Biotechnology, Agri-Food, Health, Faculty of Sciences, Sidi Mohamed Ben Abdellah University, Fez 30000, Morocco
2 Laboratory of Engineering, Electrochemistry, Modeling and Environment, Faculty of Sciences Dhar El Mahraz, Sidi Mohamed Ben Abdellah University, B.P. 1796 Atlas, Fez 30000, Morocco
3 Laboratory of Biotechnology, Conservation and Valorisation of Natural Resources (LBCVNR), Department of Biology, Faculty of Science Dhar El Mahraz, Sidi Mohamed Ben Abdellah University, B.P. 1796 Atlas, Fez 30000, Morocco
4 Laboratory of Biochemistry, Faculty of Medicine and Pharmacy, University of Sidi Mohammed Ben Abdellah, B.P. 1893, Km 22, Road of Sidi Harazem, Fez 30070, Morocco
5 Laboratory of Functional Ecology and Environment, Faculty of Sciences and Technology, Sidi Mohamed Ben Abdellah University, Imouzzer Street, P.O. Box 2202, Fez 30000, Morocco
6 Department of Zoology, College of Science, King Saud University, P.O. Box 2455, Riyadh 11451, Saudi Arabia
7 Department of Medicine and Infectious Diseases, Faculty of Veterinary Medicine, Cairo University, Giza 12211, Egypt
8 Chrono-Environnement Laboratory, UMR CNRS 6249, Franche-Comté University, CEDEX, F-25030 Besançon, France
9 Pharmacology Department, Faculty of Veterinary Medicine, Suez Canal University, Ismailia 41522, Egypt
* Correspondence: elmansouriibtissam33@gmail.com (I.E.); mohammed.kara@usmba.ac.ma (M.K.)

check for updates

Citation: Elmansouri, I.; Lahkimi, A.; Kara, M.; Hmamou, A.; Mouhri, G.E.; Assouguem, A.; Chaouch, M.; Alrefaei, A.F.; Kamel, M.; Aleya, L.; et al. A Continuous Fixed Bed Adsorption Process for Fez City Urban Wastewater Using Almond Shell Powder: Experimental and Optimization Study. *Catalysts* **2022**, *12*, 1535. https://doi.org/10.3390/catal12121535

Academic Editors: Jiangkun Du, Lie Yang and Chengdu Qi

Received: 1 October 2022
Accepted: 21 November 2022
Published: 29 November 2022

Abstract: This study deals with the valorization of a biomaterial, almond shell, for the treatment of urban effluents of the city of Fez by a fixed bed column adsorption process. A parametric analysis of the process is carried out with conditions such as particle size, pH and height of the adsorbent bed to evaluate the optimal removal percent and obtain an optimal removal capacity of the adsorbent load. Characterization of the adsorbent prior to continuous adsorption was carried out by X-ray diffraction, Fourier-transform infrared spectrometry and scanning electron microscopy. The adsorption treatment seems to be influenced by certain parameters, such as the particle size of the biomaterial used, the height of the adsorption bed and the pH. The results suggest that this biomaterial can be used as a less expensive, available, biodegradable and very effective adsorbent to eliminate the load of urban waters on a small scale and why not on a large scale to replace chemicals in the treatment and to recover waste such as almond shell. The parameters measured reached maximum values varying between 82% for COD, 79% for EC and 71% for nitrite under well-defined operating conditions, with a particle size of 0.063 mm, a height column height of 7 cm and a pH of 6.5.

Keywords: biomaterial; almond shell; urban effluents; adsorption; FTIR; XRD; SEM

1. Introduction

Pollution has increasingly become a crucial phenomenon, not only in Morocco but internationally, causing serious consequences for human health, aquatic ecosystems and animals [1].

In the context of the current situation, and compared to the pre-COVID-19 period, recent research has shown a reduction in pollution of the atmosphere, the biosphere, the hydrosphere and a clear improvement in the quality of a number of rivers. The main reason for this improvement is the decrease in industrial activity and the absence of effluents [2]. Most human activities that use water produce wastewater, and therefore, pollution levels in the natural environment are increasing alarmingly [3], negatively affecting the ecological balance, leading to serious problems and, subsequently, human health [2,4].

In this regard, the excessive demand for water in all areas allows for the production and discharge of untreated wastewater, prompting scientists to devote increased efforts to finding an approved conventional wastewater treatment method [5,6].

To face this situation of natural resources depletion and environment destruction, the orientation to wastewater treatment has become an urgent necessity; the treatment of the latter will constitute a benefit of advantage. On the one hand, it can be used as an additional renewable and reliable source of fertilizer for agriculture since it is rich in nutrients such as nitrogen and phosphorus; on the other hand, the treatment would alleviate the pressure on the conventional resources [7].

Among the different processes for the treatment of loaded effluents, adsorption is an effective and advantageous technique, which offers an economical solution by developing available, biodegradable adsorbents at a much lower cost [8].

As part of an ecological strategy, this study focuses on the reuse of solid waste based on almond shell. This biomaterial is known for its chemical composition rich in carbohydrate, proteins and minerals [9,10].

Surprisingly, several studies have been conducted on the potential application of biomaterials such as plant material, chitosan, eggshells and charcoal [2,11,12] in the treatment of wastewater instead of using chemicals that have a harmful effect on the environment and health [12].

The objective of this study is to test a new biomaterial for use in a continuous fixed-bed column adsorption process for the treatment of liquid wastes loaded with difficult-to-degrade organic matter. This study focuses on an experimental design that has been chosen to minimize experiments, errors and save time and effort, based on statistical methods that have recently received much attention in the field of environmental science and water quality modeling [7].

2. Results and Discussion

2.1. Characterization of Almond Shell

Figure 1 shows four SEM microscopic images of the surface of almond bark powder at different magnifications. The visualization of the internal microstructure shows a rather rough and irregularly shaped matrix of different sizes with the important presence of micropores and cracks well-distributed on the sample surface. This internal composition may contribute to the exchange of pollutants with the cells, thus making the adsorption mechanism more efficient [13].

Figure 2 shows that the chemical composition of almond bark used is constituted mainly of C, O and K. whose mass percentage of these elements has known high values compared to Al, Si and cl, which leads to the assumption that these elements make the adsorption mechanism more active, and this was confirmed by studies elsewhere [14].

Figure 3 is a spectrum of the X-ray diffraction (XRD) analysis of the crystal structure of almond bark, showing the intensity of the diffracted beam as a function of the detector angle. This technique is based on the collection of diffracted beams from the material to be analyzed. Examination of the spectrum shown in Figure 3 shows a diffraction peak of 20.92, corresponding to quartz (SiO_2), and a peak at 33.14 corresponding to calcite ($CaCO_3$) [15].

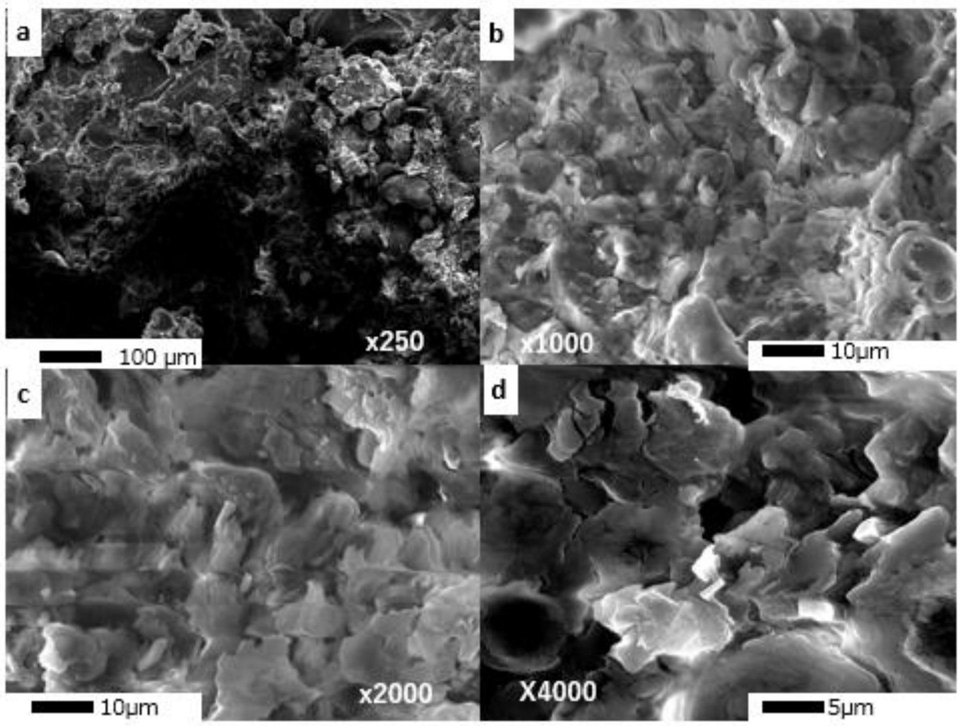

Figure 1. Scanning electron microscopy of almond bark at different magnifications: (**a**) ×250, (**b**) ×1000, (**c**) ×2000 and (**d**) ×4000.

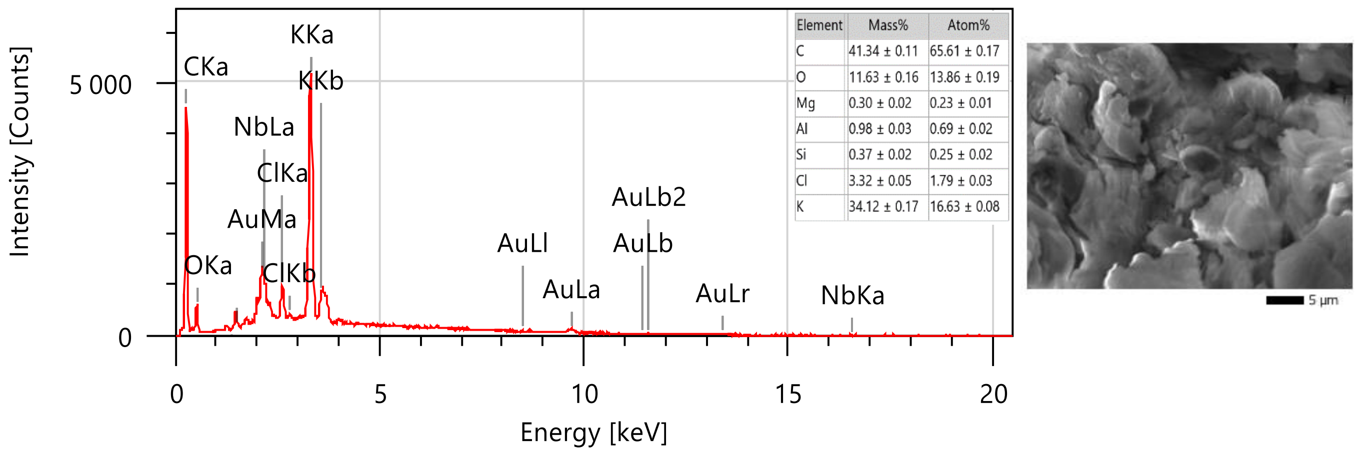

Figure 2. The different elements present in almond shell.

Figure 4 shows the evolution of transmittance in % (fraction of transmitted intensity to incident intensity) as a function of the wavenumber in cm^{-1}. From the spectrum, the intensity of the absorption peaks changes strongly. Each peak corresponds to a vibrational energy from the light absorbed from the molecule, which, in turn, corresponds to a specific chemical bond. Examination of the spectrum shown in Figure 2 shows a peak with a transmittance of 0% and a wave number of approximately 1083 cm^{-1}; this peak corresponds to a Si–O grouping [16]. The peaks located at 1411.49 cm^{-1} and 866.61 cm^{-1} certainly correspond to calcite-specific CO_3; the peak located at 3333 cm^{-1} with a transmittance of 88% corresponds to an O–H grouping [14,15].

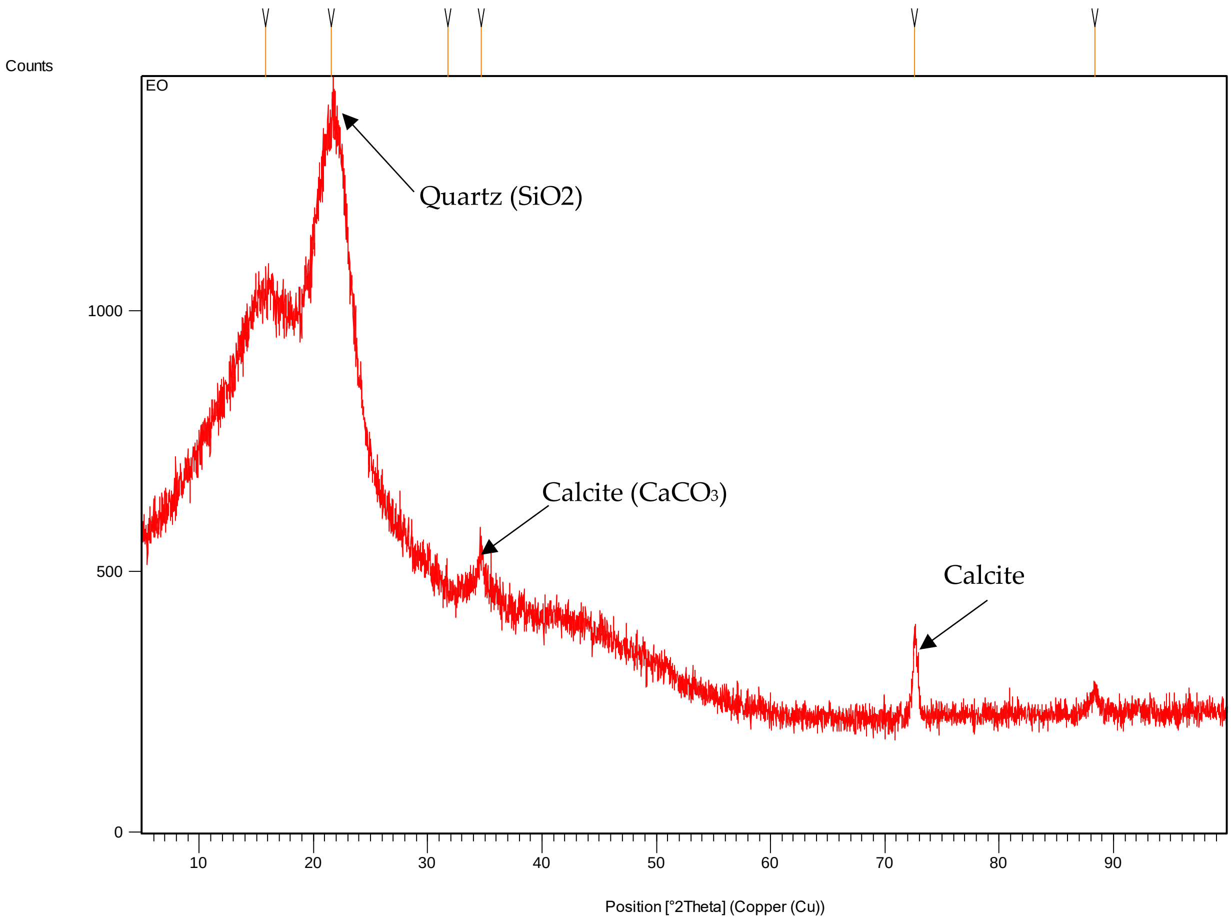

Figure 3. Crystal structure of almond bark by XRD [16].

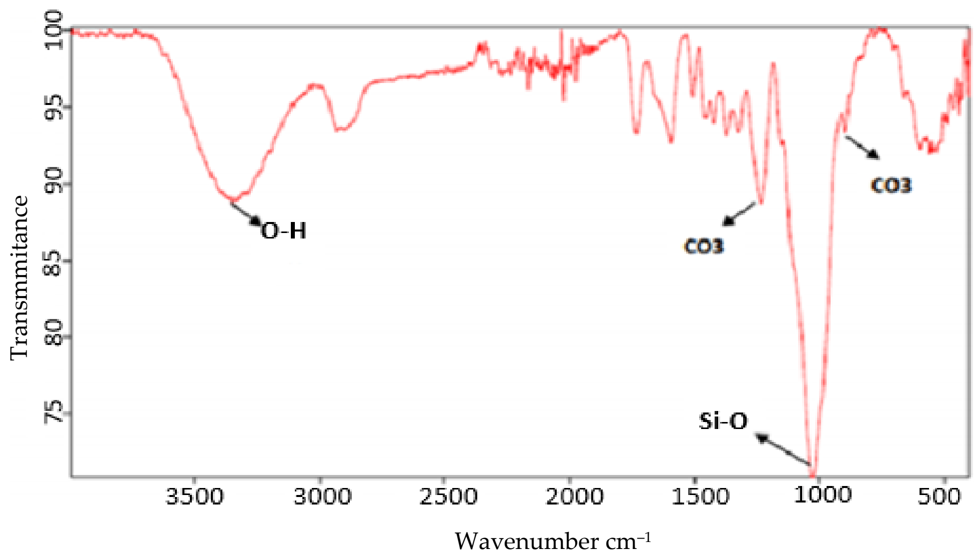

Figure 4. Infrared analysis of almond shell.

2.2. Fixed Bed Column Adsorption

The responses of the Box-Behnken optimization are shown in Table 1.

Table 1. Experimental matrix with measured responses.

Ord Essai	Granulometry (µm)	Height (cm)	pH	COD RP (%)	EC RP (%)	RP Nitrite (%)
1	281.5	7	9.0	73	73	43
2	63.0	3	6.5	79	78	53
3	281.5	5	6.5	70	72	65
4	63.0	7	6.5	82	79	71
5	500.0	5	4.0	60	45	21
6	281.5	5	6.5	70	72	65
7	281.5	7	4.0	66	72	37
8	63.0	5	9.0	78	78	56
9	500.0	3	6.5	67	48	25
10	281.5	3	4.0	68	63	56
11	281.5	5	6.5	70	72	65
12	500.0	7	6.5	73	54	25
13	500.0	5	9.0	70	52	15
14	281.5	3	9.0	75	76	43
15	63.0	5	4.0	76	64	53

2.3. Effect of Almond Shell Particle Size on the Solution pH

The pH of the effluent is measured before the treatment indicates a value of 5.4. Once this effluent has percolated through the adsorbent beds of the almond bark, an exponential increase has been observed whose height is 7 cm, and the values found are 9 and 6.5 for the 281.5 and 63 µm fractions, respectively (Table 1). Based on this data, it can be clearly seen that the pH of the raw effluent is acidic while the almond shell is basic. In fact, the value of this parameter increases according to the grain size, which can be explained by an increase in the degree of porosity, and this helps to eliminate some of the chemical elements that give the effluent its acid character. Similar research conducted by Sithole and El Mouhri [2,11] showed that the neutralization surface makes adsorption more efficient [11].

2.4. Effect of Almond Shell Particle Size on COD Reduction

Figure 5 shows the removal of organic contamination from the urban effluent in terms of COD as a function of almond bark particle size. The COD of the raw effluent has a maximum value of 1068 mg/L, but after optimization, this value decreases continuously. For the 0.500 mm fraction, the COD concentration was even higher with a value of 279 mg/L. However, when moving from one bed to another, a decrease in this value was noted, and the values found for the 0.281 and 0.063 mm fractions are 263 and 192 mg/L, respectively. Indeed, these results demonstrate the ability of the adsorption system to reduce and remove a significant amount of organic pollutants in the effluent with a removal percent of 82% (Figure 6). A similar removal percent was achieved by G. El Mouhri et al. [2] in their work on tannery adsorption by bottom ash.

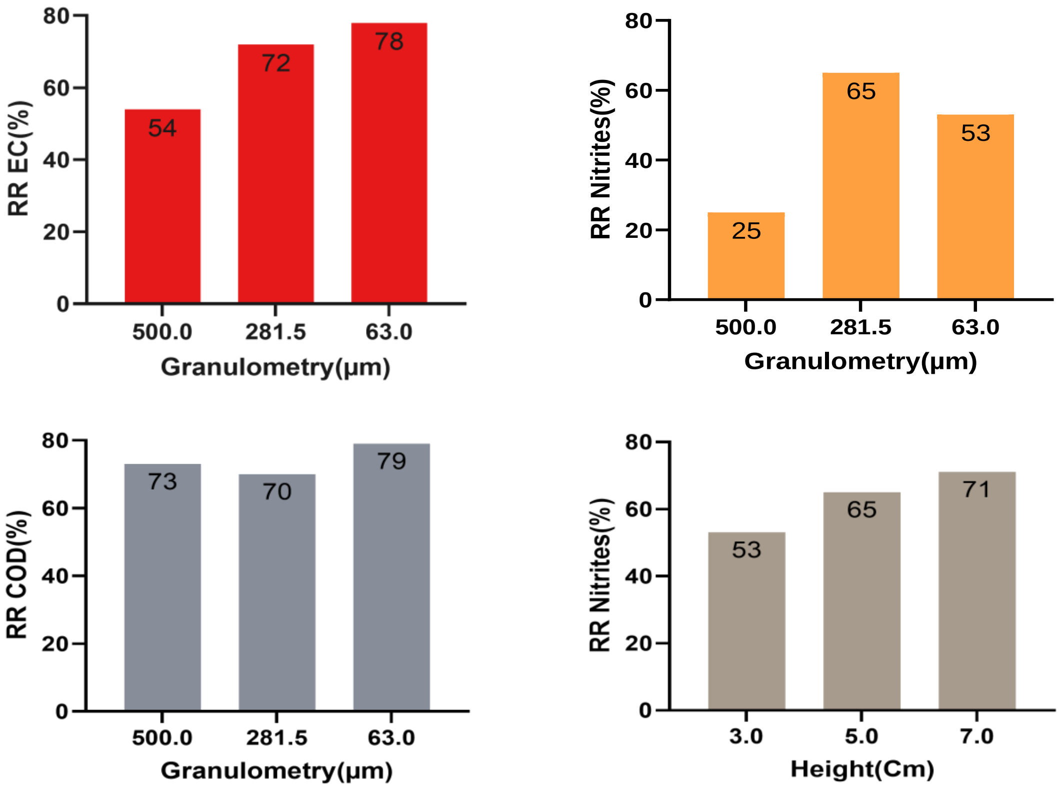

Figure 5. Parametric removal percent as a function of particle size (effluent pH = 6.5; temperature = 30 °C, particle size range between 63–500 μm; bed height = 7 cm; flow rate 20 mL.min^{-1}).

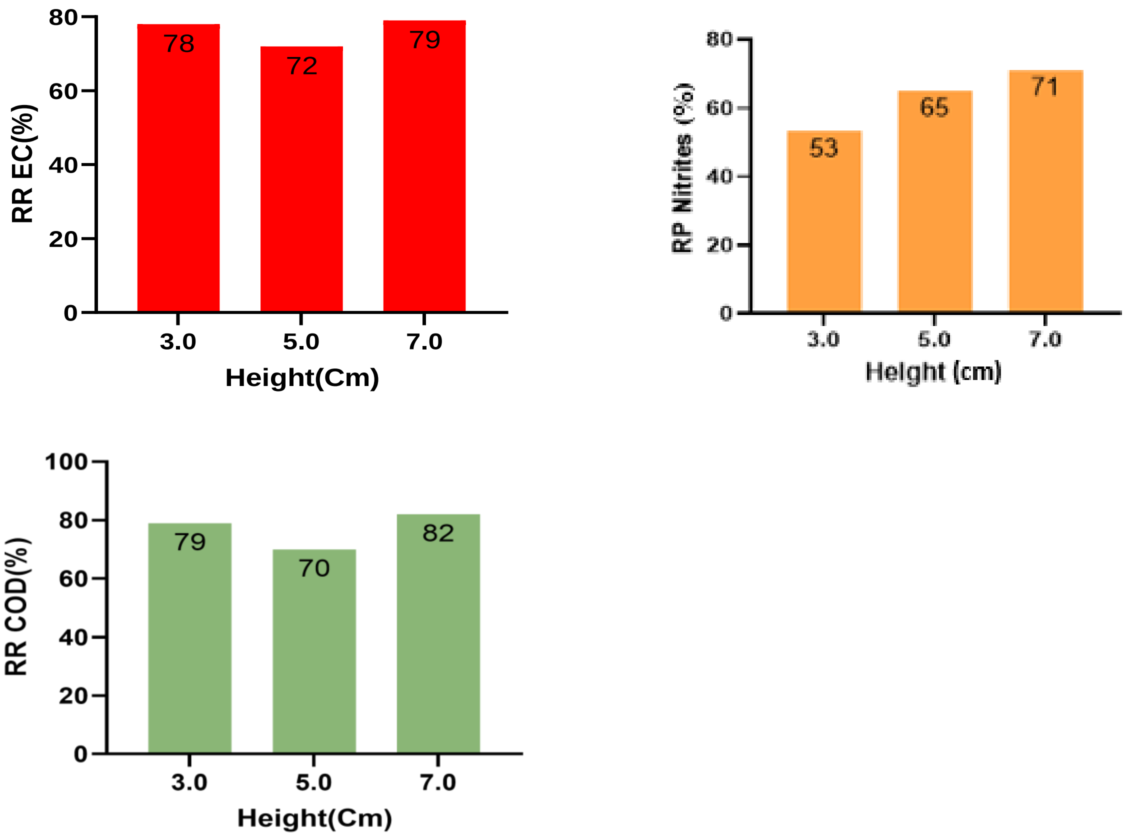

Figure 6. Parametric removal percent as a function of height (effluent pH 6.5; temperature 30 °C; height range 3–7 mm; particle size 7 cm; flow rate 20 mL/min^{-1}).

2.5. Effect of the Granulometry of Almond Shell on the Decrease of Electrical Conductivity

Figure 5 shows the electrical conductivity concentrations measured at the outlet of each column. The values obtained are approximately 2100, 1079 and 983 µs/cm for the 0.500, 0.281 and 0.063 mm fractions, respectively. From these results, it can be seen that the mineral loading of the effluent gradually decreases as the particle size decreases, compared to the value of the raw effluent. Therefore, we can conclude that fixed bed continuous adsorption with downgrading contributes to the improvement of the effluent quality in terms of electrical conductivity with a maximum abatement of about 79%. These results are almost identical to those of S. Berrada et al. [17].

2.6. Effect of Particle Size on Nitrite Removal

Figure 5 clearly shows an increase in the nitrite removal percent when moving to the smaller particle sizes. We obtained values of 24, 11 and 9 mg/L for the 0.500; 0.281 and 0.063 mm fractions. These results revealed compliance with the standards in force. The values obtained are comparable to those presented by the literature studies that have shown a positive effect of small particle sizes on treatment efficiency, resulting in a decrease in the adsorbed volume [11].

2.7. Effect of Almond Shell Size on Effluent Absorbance

Figure 5 shows the absorbance of the effluent before treatment, which reaches an excessive value of 4.973, and after percolation of the effluent through several beds of different particle sizes, there is a sharp decrease of this value to 0.952 when the particle size is equal to 0.063 mm. A progressive decrease of the absorbance percent is observed when the effluent passes successively through the three adsorbent beds and the following values are reached: 1.35 and 1.09 for the 0.500 and 0.281 mm fractions, respectively. The granulometry of the different beds determines the sizes of the pollutants trapped in both the interparticle and intraparticle spaces of the adsorbent matrix of each bed and allows for the almost complete removal of macro- and micropollutants. We can state that the granular fraction of the adsorbent is a limiting factor that needs to be optimized, so the removal capacity of fine particles is greater than that of coarse particles. This can be explained by the fact that fine particles have a large number of active sites related to the specific surface area of the material in question, which favors the rate of exchange across a large surface area [18,19]. Similar results found that a decrease in the granular size of the adsorbent had a positive impact on the availability of active sites [20,21].

2.8. Effect of Height on Parametric Reduction

From the graphical presentation in Figure 6, we can clearly see a significant reduction in pollutants with an increase in the height of the adsorbent bed to 7 cm and, therefore, an improvement in the water quality. In order to obtain an efficiency close to 82% for COD, 79% for EC and 71% for nitrite, the same adsorbent with a height of 3 and 5 decreased the removal percent less significantly, depending on the parameters measured. As the height increases, the mass of the adsorbent increases, which improves the quality of the adsorption due to the availability of active sites [22].

2.9. Continuous Adsorption Modelling Using the Experimental Design Technique

2.9.1. Box-Behnken and Statistical Analysis

This type of model is typically used in response surface methodology. The linear model terms of A (pH), B (Granulometry) and C (height); the quadratic terms of A^2 (pH×pH), B^2 (Granulometry×Granulometry) and C^2 (height×height) and the interactive model terms of AB (pH×Granulometry), AC (pH×height) and BC((Granulometry×height) show low significant values less than 0.05 [23] (Tables 2–4), as well as nonsignificant values greater than 0.05. Generally, the closer the coefficient of determination R^2 is to 1, the better the predicted model fits [1]: R^2 = 94.93% for COD, R^2 = 98.99% for EC and R^2 = 96.21% for nitrite. The empirical relationships expressed by a second-order polynomial equation that represents the behavior of the stoichiometric capacity of the column as a function of the independent variables are presented below [21] (Equations (1)–(3)):

$$\textbf{TA DCO (\%)} = 83.3 + 4.17\ \text{A} - 0.0920\ \text{B} - 6.11\ \text{C} - 0.300\ \text{AA} + 0.000060\ \text{BB} + 0.594\ \text{CC} + 0.00366\ \text{AB} - 0.000\ \text{AC} + 0.00172\ \text{BC} \quad (1)$$

$$\textbf{TA CE (\%)} = 28.2 + 11.89\ \text{A} + 0.0584\ \text{B} - 1.09\ \text{C} - 0.480\ \text{AA} - 0.000194\ \text{BB} + 0.500\ \text{CC} - 0.00320\ \text{AB} - 0.600\ \text{AC} + 0.00286\ \text{BC} \quad (2)$$

$$\textbf{TA Nitrite (\%)} = -57.4 + 24.51\ \text{A} + 0.1711\ \text{B} + 12.91\ \text{C} - 2.200\ \text{AA} - 0.000314\ \text{BB} - 1.625\ \text{CC} - 0.00412\ \text{AB} + 0.950\ \text{AC} - 0.01030\ \text{BC} \quad (3)$$

Table 2. Regression of the response surface: COD RP (%) as a function of the particle size (µm), height (cm) and pH.

Source	F-Value	*p*-Value	Remarks
Model	10.39	0.009	Significant
pH (A)	18.57	0.008	Significant
Granulometry (µm) (B)	55.63	0.001	Significant
height (cm) ©	0.69	0.445	Not significant
pH × pH (AA)	2.85	0.152	Not significant
Granulometry (mm) × Granulometry (mm) (BB)	6.71	0.049	Significant
height (cm) × height (cm) (CC)	4.58	0.085	Not significant
pH × Granulometry (mm) (AB)	3.52	0.120	Not significant
pH × height (cm) (AC)	0.00	1.000	Not significant
Granulometry (mm) × height (cm) (BC)	0.49	0.513	Not significant

Table 3. Regression of the response surface: EC RP (%) as a function of the grain size (µm), height (cm) and pH.

Source	Value of F	Value of *p*	Remarks
Model	54.67	0.000	Significant
pH (A)	40.83	0.001	Significant
Granulometry (µm) (B)	333.33	0.000	Significant
height (cm) (C)	5.63	0.064	Not Significant
pH × pH (AA)	8.86	0.031	Significant
Granulometry (mm) × Granulometry (mm) (BB)	84.25	0.000	Significant
height (cm) × height (cm) (CC)	3.94	0.104	Not Significant
pH × Granulometry (mm) (AB)	3.27	0.131	Not Significant
pH × height (cm) (AC)	9.60	0.027	Significant
Granulometry (mm) × height (cm) (BC)	1.67	0.253	Not Significant

2.9.2. Effects of Variables on the Parametric Reduction Percent

The mathematical model, which is based on the Box-Behnken methodology, made it possible to determine the main individual and interactive effects of selected process parameters with a minimum number of experiments.

In order to optimize the particle size, height and pH, the independent parameters, and the interaction of each of the two parameters on the rate of organic load reduction, were studied [23,24].

Table 4. Regression of the response surface: TA Nitrite (%) as a function of the grain size, height (cm) and pH.

Source	Value of F	Value of p	Remarks
Model	14.11	0.005	Significant
pH (A)	0.36	0.574	Not Significant
Granulometry (µm) (B)	77.95	0.000	Significant
height (cm) (C)	0.00	0.954	Not Significant
pH × pH (AA)	20.15	0.006	Significant
Granulometry (mm) × Granulometry (mm) (BB)	23.98	0.004	Significant
hauteur(cm) × height (cm) (CC)	4.50	0.087	Not Significant
pH × Granulometry (mm) (AB)	0.58	0.479	Not Significant
pH × height (cm) (AC)	2.60	0.167	Not Significant
Granulometry (mm) × height (cm) (BC)	2.34	0.187	Not Significant

The graphical presentations in Figures 5 and 6 illustrate the effects of the interactions between grain size and height and pH.

The results show that the interactions between the adsorption capacity and the variables are important and very interesting. Thus, the rate of reduction appears to be greater, with a percentage exceeding 80% when the particle size is reduced to 0.063 mm, but it can be seen that the effect is masked if the height decreases and the particle size increases, which can be attributed to the long residence time and the abundance of active sites (Figures 7 and 8) [25].

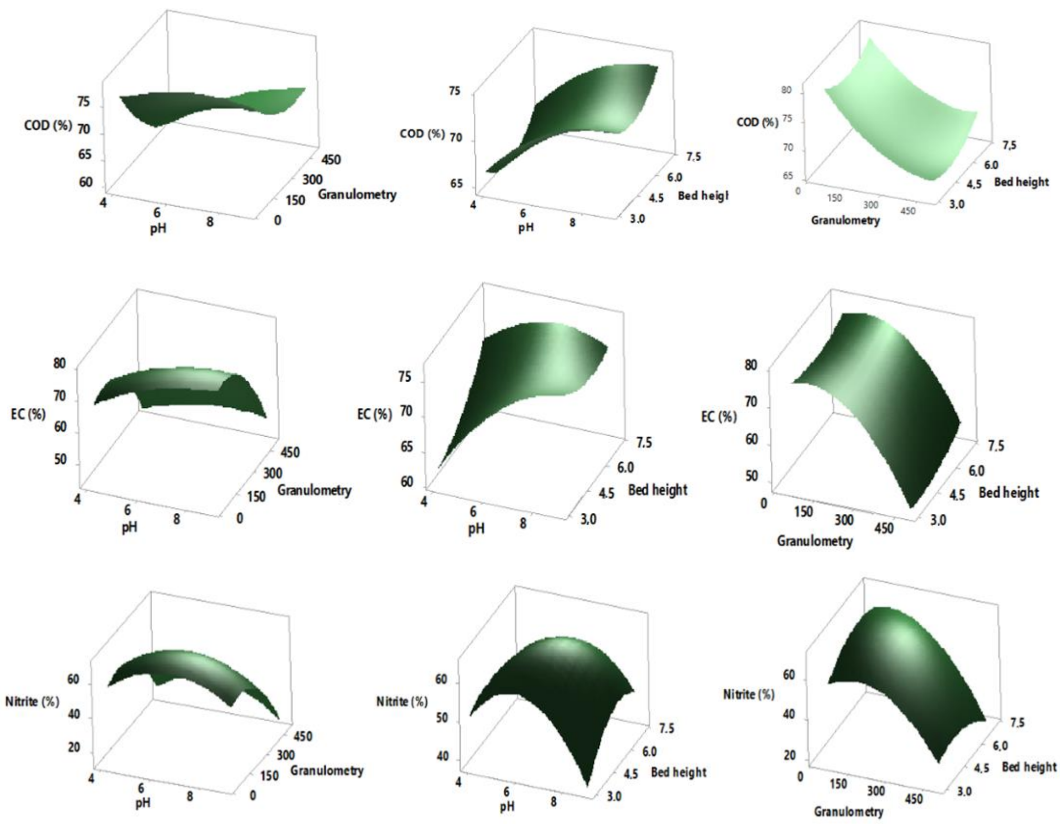

Figure 7. Surface diagram of EC RP (%), nitrite RP (%) and COD RP (%).

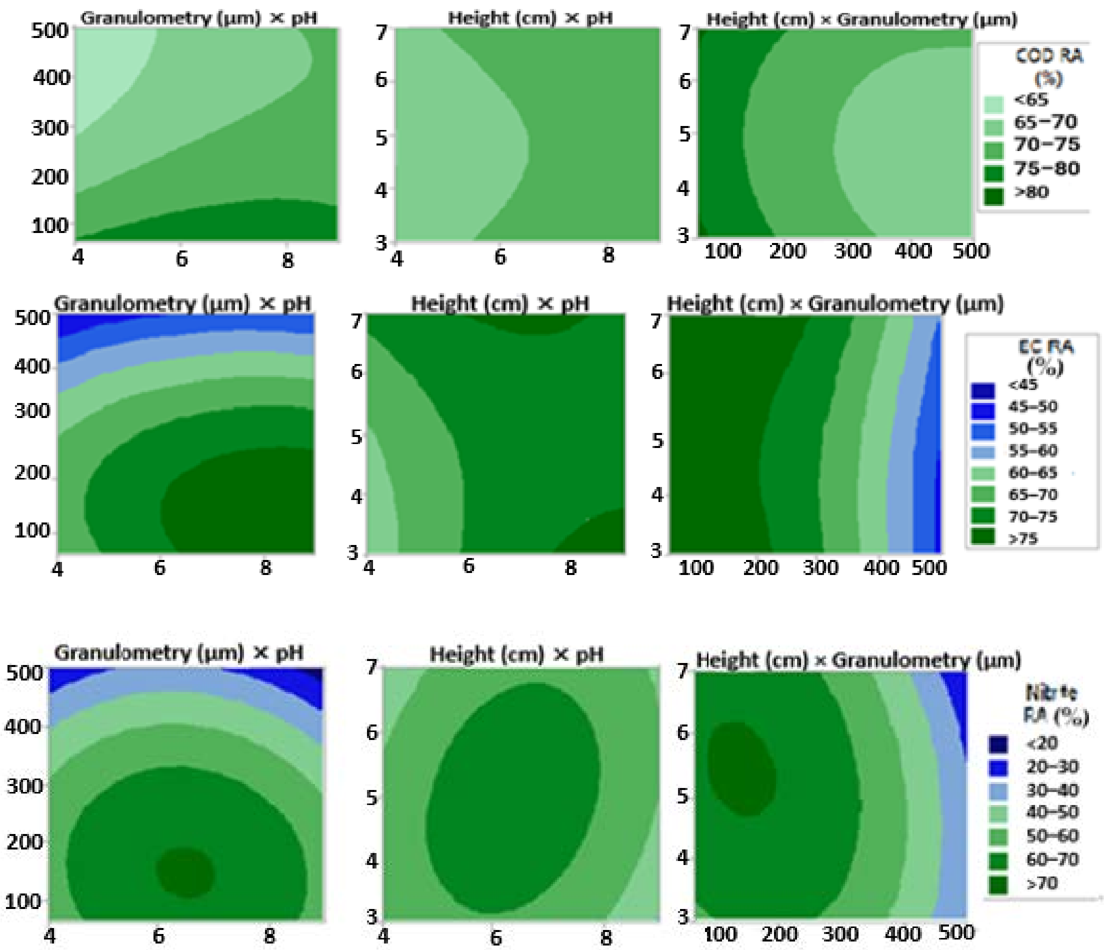

Figure 8. Contour diagram showing the effects of pH, particle size and bed height.

From Figures 7 and 8, it appears that pH plays an important role in the removal of organic load by adsorption, with significant percentage improvement observed when the pH equals 6.5. This could be attributed to several mechanisms such as electrostatic interactions, ion exchange and surface charge on carbon. The results are similar to those of Naveen Dwivedi et al. [26]. The results found are similar to those of [27], who showed that the removal percent of anionic and cationic dyes increases with increasing the adsorbent bed height. The parametric study of the process allowed a better understanding of the independent effect of each parameter on the adsorption capacity, and it was found that the adsorption quality was favored by a small size of 63µm, a height of 7 cm and pH of 6.5. It contributed to the improvement of the physicochemical quality of the effluent in terms of COD, EC, absorbance and nitrite with percentages of 80%, 75% and 70%, respectively [16,28].

3. Materials and Methods

3.1. Materials

The urban wastewater used in this study was taken from five stations (Oued El Mehraz de Sidi Brahim, Dokkarat, Oued Fès, Médina Fès and Ain Nokbi), the choice of these sampling sites for the different water samples was made taking into account the different industrial and craft activities. After the characterization of each station, and based on the measured parameters, the most polluted station, that of Ain Nokbi, is chosen to know the effectiveness of the almond shell [29].

Below is a map of the location of the study sites, which was made with QGIS software (Table 5 and Figure 9). Some parameters were measured in the field, in situ (pH, electrical conductivity, dissolved oxygen and temperature), to avoid the modification of the studied waters, while others were measured in the laboratory (COD, electrical conductivity and absorbance). For this purpose, the samples must be kept in the dark and at a temperature of 4 °C in a refrigerator; for some parameters, they must be fixed, such as COD, where a few drops of sulphuric acid were added, and for nitrites, hydrochloric acid was added [30,31].

Table 5. Geographical coordinates of the stations visited.

Stations	Geographical Coordinates
Oued Elmehraz (Station 1)	Y02°97′23″ N X99°09′13″ W
Dokkarat (Station 2)	Y04°73′47″ N X02°45′03″ W
Oued Fès (Station 3)	Y05°88′85″ N X98°99′48″ W
Medina Fès (Station 4)	Y06°65′80″ N X97°06′98″ W
Ain Nokbi (Station 5)	Y06°66′12″ N X95°25′04″ W

Figure 9. Map of the sampling stations.

The adsorbent used is an almond shell, and this adsorbent was washed several times with distilled water to eliminate any kind of adherent impurities until clear water was obtained and the pH stabilized [10], then dried in an oven for 24 h at 110 °C to avoid any alteration of the physicochemical properties of the materials and ground in a mill, allowing a powder to be obtained with homogeneous grains of small size, generally less than 2 mm; then, the particles obtained were mechanically isolated by means of a sieve (Figures 10 and 11) where the mesh size corresponded to diameters of 0.063–0.281 and 0.5 mm [32]. The identification of the nature of different components present in our material was carried out by Fourier-transform infrared spectroscopy (FTIR) (Oxford Instruments, Abingdon-on-Thames, UK) [33], the observation of the surface topography of almond shell particles was carried out by Scanning Electron Microscopy (SEM) (Oxford Instruments, Abingdon-on-Thames, UK) [2], and the determination of the crystalline structure of the materials, as well as the identification of the crystallized phases present in a biomaterial carried out by X-Ray Diffraction (XRD) (Malvern Panalytical, Malvern, UK) [34].

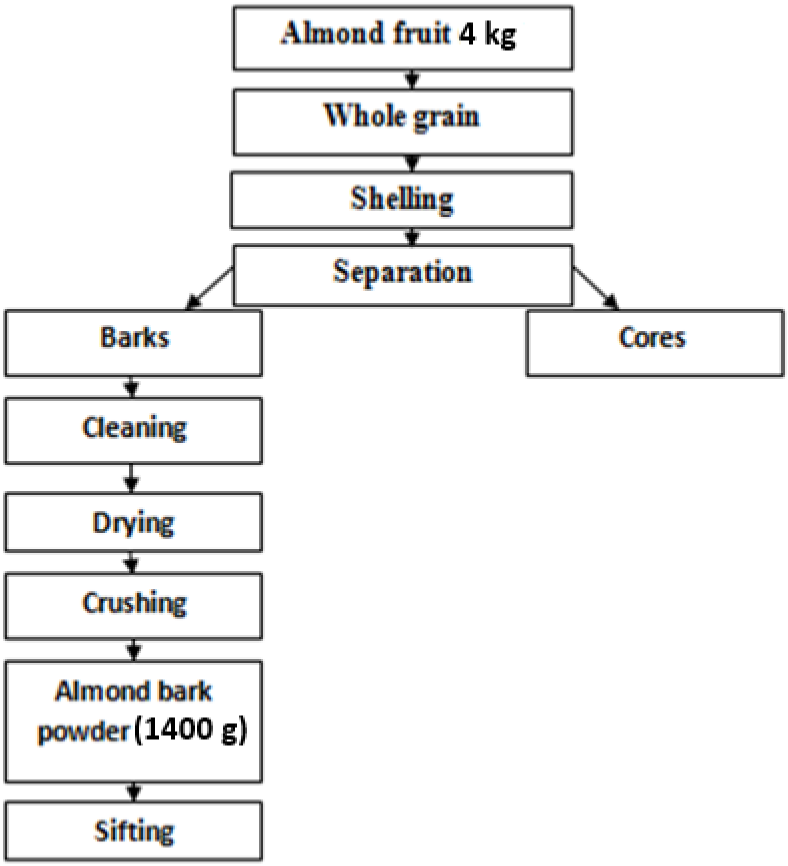

Figure 10. The different stages of almond bark powder preparation.

Figure 11. Almond bark powder with different sizes: (**a**) 0.500 mm granulometry, (**b**) 0.281 mm granulometry and (**c**) 0.063 mm granulometry.

3.2. Methods

3.2.1. Fixed Bed Column Adsorption Treatment

In this study, we used continuous fixed-bed adsorption as a treatment technique, preceded by filtration using an experimental system consisting of a glass column with an internal diameter of 3 cm and a height of 50 cm (Figure 12). The addition of the almond shell powder was done with distilled water to release the air trapped between the particles. The mass of this powder varied according to the height of the bed chosen, then a volume of 50 mL of effluent was poured for each test. In order to select the parameters that ensure better continuous adsorption (granulometry, height of the bed), a colorimetric kinetic study using a spectrophotometer (UV–Visible) (Oxford Instruments, Abingdon-on-Thames, UK) was carried out with a wavelength (λmax) of 350 nm for the most polluted station according to the characterization (Station 5) [15]. For this purpose, the effluent was percolated continuously downstream through the column, after treatment it was collected at predefined time intervals of 1 min. After the determination of the optimal granulometry, the effect of the height of the filter bed was studied to determine which one offers a better continuity of adsorption; for this purpose, the beds of bioadsorbents (powder of almond peel) were varied according to different masses; for the height of 3 cm, we worked with a mass of 6.22 g, 8.7 g for 5 cm and with 10.14 g for 7 cm. The particle size, height and pH were modified to optimize the adsorption capacity of this biomaterial under well-defined operating conditions with the adjustment of the flow rate of the effluent. The parameters ensuring a better continuous adsorption were selected using a colorimetric kinetic study at a wavelength (λmax) of 350 nm. Several parameters were measured at the outlet of each column. These parameters measured were electrical conductivity, COD, absorbance, nitrite (Table 6) and the experiment took between 2 and 3 h [2].

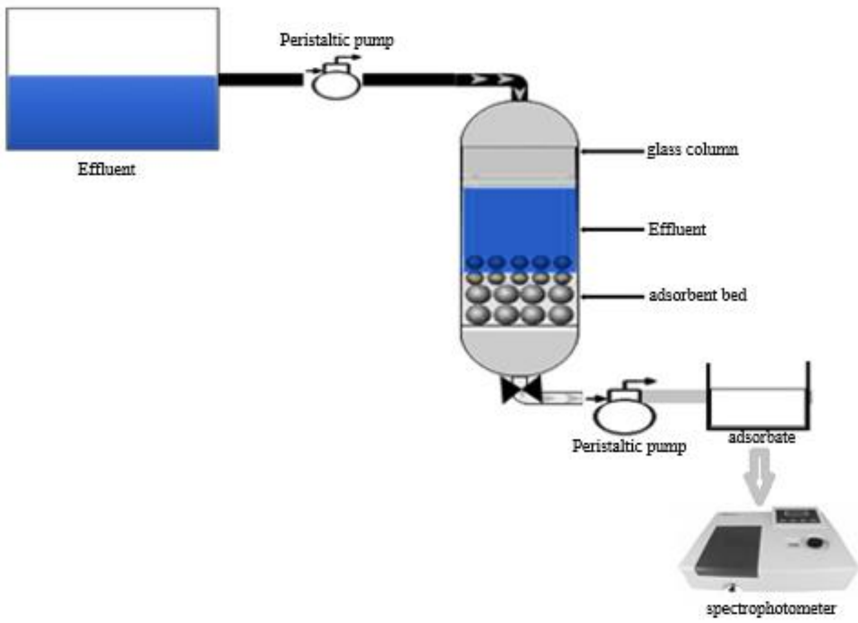

Figure 12. Experimental device of the adsorption system on a fixed bed column [15].

Table 6. Measured parameters of station 5 and equipment used.

Parameters	Values	Methods
Absorbance	4.98	Spectrophotometer UV-Visible, type Hach lange DR 3900
COD (mg of O_2/L)	1068	COD meter type hanna HI839800
BOD_5 (mg of O_2/L)	260	BOD metre type OXITOP
pH	4.6	Multiparameter HANNA HI 9829
Nitrite (mg/L)	32	Sulphosalicylic acid method
Dissolved oxygen (mg of O_2/L)	1.5	Multiparameter HANNA HI 9829
TSS (mg /L)	286	Filtration method with suction pump
Temperature (°C)	21	Multiparameter HANNA HI 9829
Electrical Conductivity (µs/cm)	4600	Multiparameter HANNA HI 9829

3.2.2. Optimization of Continuous Adsorption Using the Design of Experiments Technique

To model and analyze the continuous adsorption parameters, the response surface design, in which the response is influenced by several variables, was used to provide a mathematical model, though the Box-Behnken design, which relates the Y response to the selected factors, was applied to predict the adsorption rate (Equation (4)):

$$Y = a_0 + \Sigma a_j x_j + \Sigma a_{jj} {x_j}^2 + \Sigma\Sigma a_{jk} x_j x_j \quad (4)$$

where Y is the predicted response for the adsorption rate (%), x_j and x_k are coded independent variables and a_0, a_j, a_{jj} and a_{jk} are the intercept, linear effect, square effect and interaction effect, respectively. The measured experimental responses and the responses predicted by MINITAB 18 software with the number of experiments N = 15.

3.2.3. Fixed Bed Column Adsorption

To evaluate the effect of particle size on the treatment efficiency of plant 5, a Box-Behnken optimization was carried out to simplify it by playing on several parameters such as: pH, particle size and height (Table 7).

Table 7. Box-Behnken design variables.

Variables	Values		
pH	4	6.5	9
Granulometry (mm)	0.500	0.281	0.063
Hauteur (cm)	3	5	7

4. Conclusions

The valorization of solid wastes such as almond shell by the fixed bed continuous adsorption process was the objective in this study, which focused on the optimization of the operating performance by experimental design to better understand the effect of each parameter, such as particle size, adsorbent bed height and pH, on the adsorption capacity by taking into consideration the effluent withdrawal percent. It was found that the adsorption quality was favored by a small particle size of 63 µm, a maximum height of 7 cm and a pH of 6.5 with a minimum flow percent of 10 mL/min. Continuous adsorption with a descending granular fraction contributed to the analysis of the behavior of the urban effluent with respect to the different fractions, it contributed to the improvement of the physicochemical quality of the effluent.

The improvement of the physicochemical quality of the latter with very significant reductions in terms of COD, electrical conductivity, nitrite and adsorption were eliminated with percentages of 82%, 79%, 71% and 88%, respectively. The site development of the mathematical model based on the Box-Behnken methodology allowed the determination of the main individual effects and the interactive effects of the water, selected processes with a minimum number of experiments.

During the treatment of effluents by adsorption, there were difficulties encountered, such as clogging by the almond shell due to the granulometry.

Author Contributions: Conceptualization, I.E., A.L., G.E.M., M.C. and H.B.; Data curation, A.F.A. and L.A.; Formal analysis, A.F.A. and M.K. (Mohamed Kamel); Investigation, I.E., A.L., A.H. and A.A. (Abderrazak Adachi); Methodology, I.E., M.K. (Mohamed Kamel), N.E. and H.B.; Software, M.K. (Mohammed Kara) and A.A. (Amine Assouguem); Supervision, A.L. and H.B.; Writing—Original draft, I.E. and Writing—Review and editing, I.E., A.L., M.K. (Mohammed Kara), A.A. (Amine Assouguem) and M.M.A.-D. All authors have read and agreed to the published version of the manuscript.

Funding: This project was supported by the Researchers Supporting Project number RSP-2021/218, King Saud University, Riyadh, Saudi Arabia.

Conflicts of Interest: The authors declare no conflict of interest.

References

1. Ait Kadi, M.; Ziyad, A. Integrated water resources management in morocco. *Water Resour. Dev. Manag.* **2018**, *20*, 143–163.
2. El Mouhri, G.; Merzouki, M.; Kachkoul, R.; Belhassan, H.; Miyah, Y.; Amakdouf, H.; Elmountassir, R.; Lahrichi, A. Fixed-bed adsorption of tannery wastewater pollutants using bottom ash: An optimized process. *Surf. Interfaces* **2020**, *22*, 100868. [CrossRef]
3. Melhaoui, R.; Miyah, Y.; Kodad, S.; Houmy, N.; Addi, M.; Abid, M.; Mihamou, A.; Serghini-Caid, H.; Lairini, S.; Tijani, N.; et al. On the Suitability of Almond Shells for the Manufacture of a Natural Low-Cost Bioadsorbent to Remove Brilliant Green: Kinetics and Equilibrium Isotherms Study. Study. *Sci. World J.* **2021**, *2021*, 1–13. [CrossRef] [PubMed]
4. Tulun, Ş.; Şimşek, İ.; Bahadır, T.; Çelebi, H. Investigation of removal of anthocyanin in turnip juice wastewater by using different adsorbents. *SN Appl. Sci.* **2019**, *1*, 1–9. [CrossRef]
5. Yahya, M.D.; Obayomi, K.S.; Abdulkadir, M.B.; Iyaka, Y.A.; Olugbenga, A.G. Characterization of cobalt ferrite-supported activated carbon for removal of chromium and lead ions from tannery wastewater via adsorption equilibrium. *Water Sci. Eng.* **2020**, *13*, 202–213. [CrossRef]
6. Jawad, A.H.; Malek, N.N.A.; Abdulhameed, A.S.; Razuan, R. Synthesis of magnetic chitosan-fly ash/Fe_3O_4 composite for adsorption of reactive Orange 16 dye: Optimization by Box–Behnken design. *J. Polym. Environ.* **2020**, *28*, 1068–1082. [CrossRef]
7. Gaga, Y.; Benmessaoud, S.; Kara, M.; Assouguem, A.; Al-Ghamdi, A.A.; Al-Hemaid, F.M.; Elshikh, M.S.; Ullah, R.; Banach, A.; Bahhou, J. New Margin-Based Biochar for Removing Hydrogen Sulfide Generated during the Anaerobic Wastewater Treatment. *Water* **2022**, *14*, 3319. [CrossRef]
8. Elmountassir, R.; Bennani, B.; Miyah, Y.; Fegousse, A.; el Mouhri, G.; Oumokhtar, B.; Khatouf, M.; Elkarrach, K.; Touimi, G.B.; Lahrichi, A. Microbiological and Physicochemical Characterization of Hospital Effluents before and after Treatment with Two Types of Sawdust. *J. Chem.* **2019**, *2019*, 327510. [CrossRef]
9. Aliyu, A. Synthesis, electron microscopy properties and adsorption studies of Zinc(II) ions (Zn^{2+}) onto as-prepared Carbon Nanotubes (CNTs) using Box-Behnken Design (BBD). *Sci. African* **2019**, *3*, e00069. [CrossRef]
10. Arida, C.V.J.; De Luna, M.D.G.; Futalan, C.M. Optimization of As(V) removal using chitosan-coated bentonite from groundwater using Box—Behnken design effects of adsorbent mass, flow rate, and initial concentration. *Desalination Water Treat.* **2015**, *57*, 3994. [CrossRef]
11. Sithole, N.T.; Ntuli, F.; Okonta, F. Fixed bed column studies for decontamination of acidic mineral effluent using porous fly ash-basic oxygen furnace slag based geopolymers. *Miner. Eng.* **2018**, *154*, 106397. [CrossRef]
12. Elmansouri, I.; Lahkimi, A.; Mansour, O.; Elouadrhiri, F.; Chaouch, M.; Eloutassi, N.; Elkhamar, F.; Bekkari, H. Study of the Operation of an Industrial Water Treatment Plant of the Northern Soft Drink CompanFez, Morocco. *Ecol. Eng. Environ. Technol.* **2022**, *23*, 227–232. [CrossRef]
13. Dutta, J.; Kandhari, D. Efficacy of Almond Shells for Removal of Dye From Waste Water. *EM Int.* **2019**, *37*, 25–31.
14. Yahya, M.D.; Abubakar, H.; Obayomi, K.S.; Iyaka, Y.A.; Suleiman, B. Results in Engineering Simultaneous and continuous biosorption of Cr and Cu (II) ions from industrial tannery effluent using almond shell in a fixed bed column. *Results Eng.* **2020**, *6*, 100113. [CrossRef]
15. El Mouhri, G.; Merzouki, M.; Belhassan, H.; Miyah, Y.; Amakdouf, H.; Elmountassir, R.; Lahrichi, A. Continuous Adsorption Modeling and Fixed Bed Column Studies: Adsorption of Tannery Wastewater Pollutants Using Beach Sand. *J. Chem.* **2020**, *2020*, 1–9. [CrossRef]
16. Cemalgil, S.; Onat, O.; Tanaydın, M.K.; Etli, S. Effect of waste textile dye adsorbed almond shell on self-compacting mortar. *Constr. Build. Mater.* **2021**, *300*, 123978. [CrossRef]
17. Berrada, S.; Squalli, F.Z.; Squalli, H.T.; Hannin, M.; El Oualti, A.; El Ouali Lalami, A. Recycling of the effluents of the haemodialysis service of the Al Ghassani hospital in the city of Fez: Characterization before and after treatment. *J. Mater. Environ. Sci.* **2014**, *5*, 2265–2277.
18. Kumari, U.; Biswas, S.; Meikap, B.C. Environmental Technology & Innovation Defluoridation characteristics of a novel adsorbent developed from ferroalloy electric arc furnace slag: Batch, column study and treatment of industrial wastewater. *Environ. Technol. Innov.* **2020**, *18*, 100782.
19. Prasanna, L.; Rao, K.; Chang, Y. Chemosphere Process optimization and modeling of lead removal using iron oxide nanocomposites generated from bio-waste mass. *Chemosphere* **2020**, *243*, 125257.
20. Peter, C.; Olufemi, G.; Zhang, Q.; Zhu, G.; Wang, C.; Guo, Q. Aqueous scavenging of polycyclic aromatic hydrocarbons using epichlorohydrin, diphenyl diisocyanate modified starch: Pollution remediation approach. *Arab. J. Chem.* **2019**, *12*, 2760–2773.
21. Elassassi, Z.; Ougrad, I.; Bedoui, I.; Kara, M.; El Bouch, M.; Assouguem, A.; Fadli, M.; Almeer, R.; Mohamed, H.R.H.; Peluso, I.; et al. Spatial and Temporal Variations of the Water Quality of the Tiflet River, Province of Khemisset, Morocco. *Water* **2022**, *14*, 1829. [CrossRef]
22. Jafari, A.; Mahvi, A.H.; Nasseri, S.; Rashidi, A.; Nabizadeh, R.; Rezaee, R. Environmental Health Ultrafiltration of natural organic matter from water by vertically aligned carbon nanotube membrane. *J. Environ. Health Sci. Eng.* **2015**, *13*, 1–9.
23. Sugashini, S.; Begum, K.M.M.S. Column Adsorption Studies for the Removal of Cr (VI) Ions by thylamine Modied Chitosan Carbonized Riceus Composite Beads with Modelling and Optimization. *J. Chem.* **2013**, *2013*, 460971. [CrossRef]

24. Mourabet, M.; El Rhilassi, A.; El Boujaady, H.; El Hamri, R.; Taitai, A. Applied Surface Science Removal of fluoride from aqueous solution by adsorption on Apatitic tricalcium phosphate using Box—Behnken design and desirability function. *Appl. Surf. Sci.* **2012**, *258*, 4402–4410. [CrossRef]
25. Reske, G.D.; da Rosa, B.C.; Visioli, L.J.; Dotto, G.L.; De Castilhos, F. Intensification of Ni(II) adsorption in a fixed bed column through subcritical conditions. *Chem. Eng. Process. Process Intensif.* **2020**, *149*, 107863. [CrossRef]
26. Dwivedi, N.; Balomajumder, C.; Mondal, P. Study for the treatment of Cyanide bearing Wastewater using Bioadsorbent Prunus Amygdalus (Almond shell): Effect of pH, adsorbent dose, Contact Time, Temperature, and initial Cyanide concentration. *Int. Res. J. Environ. Sci.* **2014**, *3*, 23–30.
27. Akazdam, S.; Chafi, M.; Yassine, W.; Sebbahi, L.; Gourich, B.; Barka, N. Adsorption on NaOH treated eggshells: Batch and fixed bed column study using Response Surface Methodology Decolourization of Cationic and Anionic Dyes from Aqueous Solution by Adsorption on NaOH Treated Eggshells: Batch and Fixed Bed Column Study using response surface methodology. *J. Mater. Env. Sci.* **2017**, *8*, 784–800.
28. Estevinho, B.N.; Ribeiro, E.; Alves, A.; Santos, L. A preliminary feasibility study for pentachlorophenol column sorption by almond shell residues. *Chem. Eng. J.* **2008**, *136*, 188–194. [CrossRef]
29. Elmansouri, I.; Lahkimi, A.; Benaabou, M.; Chaouch, M.; Eloutassi, N.; Bekkari, H. Contribution to the Treatment of Urban Wastewater in the City of Fez by Coagulation and Flocculation Using a Biodegradable Reagent. *J. Ecol. Eng.* **2022**, *23*, 77–85. [CrossRef]
30. Adachi, A.; Ouadrhiri, F.E.; Kara, M.; El Manssouri, I.; Assouguem, A.; Almutairi, M.H.; Bayram, R.; Mohamed, H.R.H.; Peluso, I.; Eloutassi, N.; et al. Decolorization and Degradation of Methyl Orange Azo Dye in Aqueous Solution by the Electro Fenton Process: Application of Optimization. *Catalysts* **2022**, *12*, 665. [CrossRef]
31. Rodier, J.; Legube, B.; Merle, N. *Water Analysis*, 9th ed.; DUNOD: Paris, France, 2009; p. 1600.
32. Azoulay, K.; Bencheikh, I.; Moufti, A.; Dahchour, A.; Mabrouki, J.; El, S. Comparative study between static and dynamic adsorption efficiency of dyes by the mixture of palm waste using the central composite design. *Chem. Data Collect.* **2020**, *27*, 100385.
33. Magdziarz, A.; Dalai, A.K.; Koziński, J.A. Chemical composition, character and reactivity of renewable fuel ashes. *Fuel* **2016**, *176*, 135–145. [CrossRef]
34. Shi, R.; Li, J.; Jiang, J.; Mehmood, K.; Liu, Y.; Xu, R.; Qian, W. Characteristics of biomass ashes from different materials and their ameliorative effects on acid soils. *JES* **2016**, *55*, 294–302. [CrossRef] [PubMed]